Inventory of supplementary materials submitted:

Supplementary methods and corresponding references

Supplementary figures (9)

Supplementary figure legends

Supplementary table 1

Supplemetary table 2

Supplementary methods:

Genotyping of genetically-modified mice: Genotyping was done on mouse genomic tail DNA using primers to detect GluA1 flox allele : for sense strand 5`- CAC TCA CAG CAA TGA AGC AGG AC-3` and for anti-sense 5- CTG CCT GGG TAA AGT GAC TTG G -3`; to detect GluA2 flox allele : for sense strand 5`- GTT GTC TAA CAA GTT GTT GACC-3` and for anti-sense strand 5`- GAA TCA TTG TTG ACA GAT TGC CAC-3`; and to detect SNS-Cre transgene expression: for sense strand 5`- GAA AGC AGC CAT GTC CAA TTT ACT GAC CGT AC -3` and for anti-sense 5- GCG CGC CTG AAG ATA TAG AAG A -3`.

Immunohistochemistry: Mice were perfused transcardially with 4% paraformaldehyde (PFA) and spinal cords, brains or dorsal root ganglia were extracted and postfixed for up to 18 hours (5 hours, in case of the anti-PSD95 antibody) in 4% PFA. Immunohistochemistry was performed on Vibratome sections (50 µm) or cryosections (20 µm) using standard reagents and protocols (Vector Laboratories, Burlingame, USA). Sections from treatment groups to be compared were stained and photographed together and care was taken to ensure that the staining reaction was within the linear range. Brightfield images were taken under similar illumination conditions. For quantification of ERK-phosphorylation in DRG neurons, pERK-

positive cells were counted in at least 5 sections/DRG and at least 2 DRGs/mouse before data was averaged for that respective mouse. TRITC-conjugated streptavidin (Vector Laboratories) and FITC-conjugated anti-rabbit secondary antibody were used to detect biotinylated Isolectin-B4 and CGRP, respectively, which were visualized using a laser-scanning confocal microscope TCS-AOBS (Leica, Bensheim, Germany).

For analysing synaptic contacts in spinal cord sections, following incubation with a guinea pig anti-CGRP antibody or biotinylated IB4, signal amplification with Tyramide signal amplification rhodamine kit was performed, followed by antigen retrieval using pepsin treatment. Sections were then processed for staining with a rabbit PSD-95 antibody described by Fukaya et al. (1) (a generous gift from M. Watanabe) and visualized with an Alexa488 secondary antibody. Confocal images were analysed by selection of 100 CGRP-positive boutons and 50 IB4-positive boutons per animal and subsequent quantification of PSD-95 positive puncta in contact with these. Results are expressed as percentage of boutons with at least one contact and mean number of contacts per bouton.

Nociceptive tests and mouse models of acute and chronic pain: Determination of latency of paw withdrawal in response to noxious heat and graded pressure was done using the plantar test apparatus (Ugo Basile, Italy), as described by Hargreaves (2), with a sensitivity of 0.1s (n = 7-14 per group). Mechanical sensitivity was tested in the same cohort of animals via manual application of von Frey hairs to the plantar surface and via the use of an automated Dynamic aesthesiometer (Ugo Basile Inc.) as described previously (3). Complete Freund's adjuvant (CFA) was injected unilaterally in the intraplantar surface of the hindpaw in mice (30 µl), whereas control mice were injected with 0.9% saline, as described in details previously (3).

Dimensions of the each hindpaw were recorded before and at intervals after CFA injection were measured using a fine calliper and paw oedema was calculated as a change in paw volume (length X width X height) as well as by using a Plethysmometer, as described in detail by Cirino et al. (4).

Formalin (1%, 20 µl) or capsaicin (0.06%, 10 µl) was injected into the plantar surface of the right hindpaw and the duration of nocifensive behaviours including lifting, licking or flinching of the injected paw was measured for 5 min after capsaicin injection or in 5 min bins for 50 min after formalin injection as described previously (5,6).

To induce knee arthritis, mice were anesthetisized by intraperitoneal injection of ketamin (120 mg/kg) and xylazin (16 mg/kg) and 30 µl of a 4% kaolin solution were injected intra-articularly through the ligamentum patellare followed by a period of 15 min in which the knee was manually bent and straightened, as described by Bar et al. (7). Subsequently, 30 µl of a 2% Carrageenan solution were injected and the knee again moved for 5 min. This treatment causes inflammation and swelling of the knee within 1 to 3 hours that lasts for about 2 weeks without systemic spreading (7). The resulting mechanical hyperalgesia was measured every second day over 8 days in total using von Frey filaments as described above. To assess the severity of edema formation and inflammation, circumference of the knee joint was measured with a tape measure prior to injections and following every determination of paw withdrawal latencies.

In order to exclude motor deficits caused by GYKI 52466 injections mice were tested in the Open Field test as described previously (8). An area of 40 x 40 cm was subdivided into squares of 8.5 x 8.5 cm and surrounded with wooden walls. Mice were put in the centre of the field and then observed for 10 min. The number of times the animals crossed the outlines of the squares (horizontal activity) was counted as

well as the number of rearings (vertical activity). Naïve animals were compared to mice which received either intraplantar (5 nmol) or subcutaneous (20 µmol/kg) injections of GYKI 52466.

Skin-nerve preparation and single-fiber recordings: Animals were killed by exposure to a rising concentration of CO_2 gas. After shaving the hindlimb, the skin from the area innervated by the saphenous nerve was removed with the nerve intact. After dissection the preparation was placed in a bath chamber with the corium side of the skin facing up to ensure efficient oxygenation. The preparation was superfused with an oxygen-saturated modified synthetic interstitial fluid (SIF) solution containing (mM): 123 NaCl, 3.5 KCl, 0.7 $MgSO_4$, 1.7 NaH_2PO_4, 2,0 $CaCl_2$, 9.5 sodium gluconate, 5.5 glucose, 7.5 sucrose and 10 *N*-2-hydroxyethylpiperazine- *N'*-2-ethanesulfonic acid (HEPES), adjusted to pH 7.4±0.05, temperature, 32±0.5. The saphenous nerve was desheathed and individual filaments teased away enabling extracellular recordings to be made from functionally identified single fibers. All data described in this paper are from functionally single fibres. To ensure this was the case a template of the spike under study was saved on the oscilloscope (Tektronix TDS 200) and evoked spikes visually monitored to make sure that no other active spikes would be mistaken for the one under study. The powerlab system and Chart 5 software (AD Instruments, Germany) was used for data acquisition and analysis.

The receptive fields of identified fibers were found by probing the skin with a glass rod. In this way up to 90% of thin myelinated or unmyelinated nociceptors and virtually all of the low-threshold mechanoreceptors can be activated (9). Once the borders of the receptive field were determined, a Teflon-coated steel electrode wave inserted into the receptive field and the conduction velocity of the afferent determined by electrical stimulation. Units with conduction velocities of < 1m/s were classified as

unmyelinated C-fibers; those with conduction velocities of between 1 and 10 m/s were classified as thin myelinated sensory afferent Aδ-fibers (10). Low–threshold mechanoreceptors with Aβ-fibres usually had conduction velocities of >10m/s. The mechanical threshold was established using calibrated von Frey hairs applied perpendicular to the receptive field. The weakest von Frey filament in this study exerted a bending force of 0.4 mN. After electrical stimuli, by using a probe fixed to a linear stepping motor under computer control (Nanomotor, Kleindiek Nanotechnic), a standard ascending series of displacement stimuli were applied to the receptive field at 30s intervals and each displacement was maintained for 10s as described in details by (11, 12). Each stimulus-response function started at threshold as the probe was adjusted so that the first 6 µm displacement evoked spikes. The delay between the start of the mechanical probe movement and the first spike, corrected for the electrical conduction delay of the tested fiber, was designated as the mechanical latency. For noxious heat stimulation of nociceptors the method was essentially identical to that described by Milenkovic et al. (13); a thermocouple was placed on the corium surface of the skin over the receptive field of an identified C-fiber nociceptor. The temperature was ramped between 32 and 52 °C (rate 1^{o}C/s). The threshold for the first and second spikes was measured on the rising phase of the ramp and the firing frequency was measured during both rising and falling phases during temperature change.

For the application of capsaicin, a metal ring (diameter = 8mm) was used to isolate the receptive field and 100µl of capsaicin was applied in buffer solution within the metal ring for 200s. This method was essentially as described previously (13).

Microdialysis of glutamate levels in the spinal cord: A probe was built from a hollow fibre (polyacrylonitril; AN69, ∅ 200µm, cut-off at. 40kDa; Hospal, Germany), with an

inner PE-tube (∅i 0.26µm, ∅o 0.6µm). This catheter was introduced into the lumbar spinal cord via the vertebral joints as described by Ates et al. (14). Anaesthesia was switched from isoflurane to urethane during the dialysis. The probe was connected to a pump and perfused with carbogenated ACSF at a speed of 1.5µl/min (ACSF: 141.7mM Na^+, 2.6mM K^+, 0.9mM Mg^{2+}, 1.3mM Ca^{2+}, 122.7mM Cl^-, 21mM HCO_3^-, 2,5mM HPO_4^{2-} und 3.5mM dextrose; pH 7,2). Samples were directly collected from the hollow fibre. After 2 hours of equilibration basal values were measured over 12 intervals of 5 min each. Following the bilateral injection of 20µl formalin into the plantar surface of the hindpaws, dialysis samples were collected for another 12 intervals of 5 min each, kept on ice and processed within 15 min after extraction. The glutamate content was determined by using a CMA 600 Analyzer (CMA Stockholm, Sweden) according to the manufacturer's protocol. The correct placement of the catheter within the L4 dorsal horn was finally assessed under a microscope. Glutamate concentrations were averaged over all animals in one group per time-point or expressed as area-under-the-curve (AUC).

Calcium imaging from cultured DRG neurons: Mice (6-8 weeks old) were killed by inhalation of CO_2. Bilateral spinal ganglia were removed in DMEM solution. DRG neurons were dissociated and plated on coverslips precoated with poly-lysine. At 24-48 h after culture, neurons were loaded with Fura-2 (10 µM) for 30 min. After 30 min of de-esterification period, neurons were incubated with a vital marker, Alexa 488 conjugated IB4 (10 µg/ml; Molecular probes) for live identification of small-diameter neurons for 10 min and washed in bathing solution before Ca^{2+} imaging. This step was necessary because the DRG cultures represent a heterogeneous mix of different types of sensory neurons, whereas the gene deletion only occurs in nociceptors in the mice analysed here. Calcium signals were recorded at a rate of 1 Hz using an

upright fluorescence Olympus BX51WI microscope (Olympus, Japan) with 10X objective, a Sensicam CCD camera (PCO) and TILLvisION (T.I.L.L. Photonics). Agonists were applied by bath application for 10-20 sec and a 10 -15 min washout interval was employed between subsequent applications. F340/380 ratios were calculated as described previously (15).

Patch-clamp recordings on mouse spinal cord slices: Mice were anesthetized with halothane at postnatal days 15-21 and decapitated, the spinal cord and vertebrae were rapidly removed and placed in ice-cold Krebs' solution (composition in mM:125 NaCl, 2.5 KCl, 1.25 NaH_2PO_4, 26 $NaHCO_3$, 25 glucose, 1 $MgCl_2$, and 2 $CaCl_2$, pH 7.4, 320 mOsm), bubbled with carboxygen (95% O_2, 5% CO_2). The lumbar part of the spinal cord was isolated, laid down on an agarose block, and transverse slices (500 µm thick) with dorsal roots attached were obtained using a vibrating microtome (Campden Instruments, UK). Slices were incubated in oxygenated Krebs' solution at 35°C for 1 hour and used for recording within 6-7 h.

Patch-clamp recording in whole-cell configuration was performed on visually identified lamina I and II neurons at room temperature. Neurons were visualized by using a Zeiss Axioskop microscope, fitted with Nomarski optics and connected to a camera (Dage-MTI, USA). Slices were perfused at 1-2 ml/min. Recordings were performed in voltage-clamp, at the holding potential of -80 mV. Thick-walled borosilicate pipettes, having a resistance of 3-5 mOhm, were filled with a solution having the following composition (in mM): 130 Cs-gluconate, 10 CsCl, 11 EGTA, 1 $CaCl_2$, 10 HEPES, and 2 Mg^{2+}-ATP, pH adjusted to 7.2 with NaOH, osmolarity adjusted to 305 with sucrose. Junction potential was corrected after recording. Data were recorded and acquired using a Multiclamp 700A amplifier and pClamp 9

software (Molecular Devices, USA). Sampling rate was 10 kHz, and data were filtered at 2 kHz. Evoked EPSCs were obtained by stimulating the dorsal root with a suction electrode; stimulus intensities (set just above the threshold of the synaptic response) varied from 50 to 500 μA, stimulus duration was 0.1 ms. In order to isolate AMPA mediated EPSCs (the contribution of NMDA receptors at these holding potentials being negligible), GABA and glycinergic inputs were blocked via 10 μM bicuculline and 3 μM strychnine, respectively. Evoked EPSCs with constant latency and no failures during a train of 20 stimuli at 2 Hz were considered monosynaptic and tested for AMPA-evoked responses. Series of 100 EPSCs were evoked in control, AMPA and wash, at the frequency of 0.25 Hz. Because AMPA can also act as agonist of kainate receptors, the kainate receptor desensitizing agonist SYM 2081 (3 μM) was always present during the experiment.

Analysis of peak amplitudes of evoked EPSCs was performed by using Clampfit (pClamp9, Molecular Devices, USA). Graphs and statistical analysis were obtained by using Sigmaplot 8 (SPSS, USA). EPSC peaks were manually detected for each trace, in the same 2 ms window. Coefficient of variation (CV) of EPSC amplitudes was determined as standard deviation/mean, considering 60-70 traces for each condition.

Patch clamp recording from isolated adult DRG neurons. DRG neurons from SNS-GluA1-/- mice and GluA1fl/fl mice were dissected and collected in Ca2+ and Mg2+-free PBS and treated with collagenase IV (1mg/ml, Sigma-Aldrich) for 30min at 37°C, and trypsin (0.05%, Invitrogen, Karlsruhe, Germany,) for 30 min at 37°C. Digested DRGs were washed twice with growth medium [DMEM-F12 (Invitrogen) supplemented with L-glutamine (2mM, Sigma-Aldrich), Glucose (8mg/ml, Sigma-Aldrich), Penicilin (200U/ml)– Streptomycin (200μg/ml) (both Sigma) and 5% horse

serum (PPA)], triturated using fire-polished Pasteur pipettes and plated in a droplet of growth medium on a glass coverslip precoated with 100µg/ml poly-L-lysine (20µg/cm², Sigma-Aldrich) and 20µg/ml laminin (4µg/cm², Invitrogen). To allow neurons to adhere, coverslips were kept for 4 hours at 37°C in a humidified 5% incubator before adding fresh medium. Cultures were used for patch-clamp experiments on the next day.

Patch clamp recordings using the whole cell configuration were made at room temperature (20-24°C) from cultures prepared as described above. Patch pipettes were pulled (Flaming-Brown puller, Sutter Instruments, Novato, CA, USA) from borosilicate glass capillaries (Hilgenberg, Malsfeld, Germany), filled with a solution consisting of (mM) KCl (110), NaCl (10), MgCl2 (1), EGTA(1) and HEPES (10), adjusted to pH 7.3 with KOH and had tip resistances of 6-8MΩ. The bathing solution contained (mM) NaCl (140), KCl (4), CaCl2 (2), MgCl2 (1), glucose (4), HEPES (10), adjusted to pH 7.4 with NaOH. All recordings were made using an EPC-9 amplifier (HEKA, Lambrecht, Germany) in Patchmaster© software (HEKA). Pipette and membrane capacitance were compensated using the auto function of Patchmaster. For determination of nociceptors, action potentials were evoked by repetitive 80ms current injections increasing from 20pA to 400pA in increments of 20pA. The amount of current required for the first action potential was measured as threshold current. For excitability measurements a 2s current ramp ranging from 200pA to 1000 pA was injected to the cell soma**.**

References for supplementary methods:

1. Fukaya M, Watanabe M. Improved immunohistochemical detection of postsynaptically located PSD-95/SAP90 protein family by protease section

pretreatment: a study in the adult mouse brain. *J Comp Neurol.* 2000;426:572-86.

2. Hargreaves KM, Dubner F, Brown F, Flores C, Joris J. A new and sensitive method for measuring thermal nociception in cutaneous hyperalgesia. *Pain.* 1998;32:77.
3. Hartmann B, Ahmadi S, Heppenstall P, Zeilhofer HU, Lewin G, Schott C, Seeburg PH, Sprengel R, Kuner R. The AMPA receptor subunits, GluA1 and GluA2 reciprocally modulate spinal synaptic plasticity and inflammatory pain. *Neuron*. 2004;44:637-650.
4. Cirino G, Peers SH, Wallace JL, Flower RJ. A study of phospholipase A2-induced oedema in rat paw. *Eur J Pharmacol.* 1989;166:505-510.
5. Laird JMA Roza C, De Felipe C, Hunt SP, Cervero F. Role of central and peripheral tachykinin NK1 receptors in capsaicin-induced pain and hyperalgesia in mice. *Pain.* 2001;90:97-103.
6. Tjolsen A, Berge OG, Hunskaar S, Rosland JH, Hole K. The formalin test: an evaluation of the method. *Pain.* 1992;51:5-17.
7. Bar KJ, Natura G, Telleria-Diaz A, Teschner P, Vogel R, Vasquez E, Schaible HG, Ebersberger A. Changes in the effect of spinal prostaglandin E2 during inflammation: prostaglandin E (EP1-EP4) receptors in spinal nociceptive processing of input from the normal or inflamed knee joint. *J Neurosci.* 2004 24, 642-651.
8. Tappe A, Kuner R. Regulation of motor performance and striatal function by synaptic scaffolding proteins of the Homer1 family. *Proc Natl Acad Sci U S A.* 2006;103:774-779.

9. Kress M, Koltzenburg M, Reeh PW, Handwerker HO. Responsiveness and functional attributes of electrically localized terminals of cutaneous C-fibers in vivo and in vitro. *J Neurophysiol*. 1992;68:581-595.
10. Koltzenburg M, Stucky CL, Lewin GR. Receptive properties of mouse sensory neurons innervating hairy skin. *J Neurophysiol.* 1997;78:1841-50.
11. Milenkovic N, Frahm C, Gassmann M, Griffel C, Erdmann B, Birchmeier C, Lewin GR, Garratt AN. Nociceptive tuning by stem cell factor/c-Kit signalling. *Neuron.* 2007;56(5):893-906.
12. Milenkovic N, Wetzel C, Moshourab R, Lewin GR. Speed and temperature dependences of mechanotransduction in afferent fibers recorded from the mouse saphenous nerve. J Neurophysiol. 2008;100(5):2771-83.
13. Park TJ, Lu Y, Jüttner R, Smith ES, Hu J, Brand A, Wetzel C, Milenkovic N, Erdmann B, Heppenstall PA, Laurito CE, Wilson SP, Lewin, GR. Selective inflammatory pain insensitivity in the African naked mole-rat (Heterocephalus glaber). *PLoS Biol.* 2008;6(1):e13.
14. Ates M, Hamza M, Seidel K, Kotalla, CE, Ledent C, Gühring H. Intrathecally applied flurbiprofen produces an endocannabinoid-dependent antinociception in the rat formalin test. *Eur J Neurosci*. 2003;17(3):597-604.
15. Luo C, Seeburg PH, Sprengel R, Kuner R. Activity-dependent potentiation of calcium signals in spinal sensory networks in inflammatory pain states. *Pain.* 2008;140:358-67.

Supplementary Figure 1: Immunohistochemical determination of expression of GluA1 and GluA2 subunits in specific subsets of DRG neurons in SNS-GluA1$^{-/-}$ mice and the corresponding GluA1$^{fl/fl}$ controls. Peptidergic nociceptors are identified via binding to isolectin-B4 (IB_4) and non-peptidergic nociceptors are identified via expression of CGRP. Scale bars represent 50 µM.

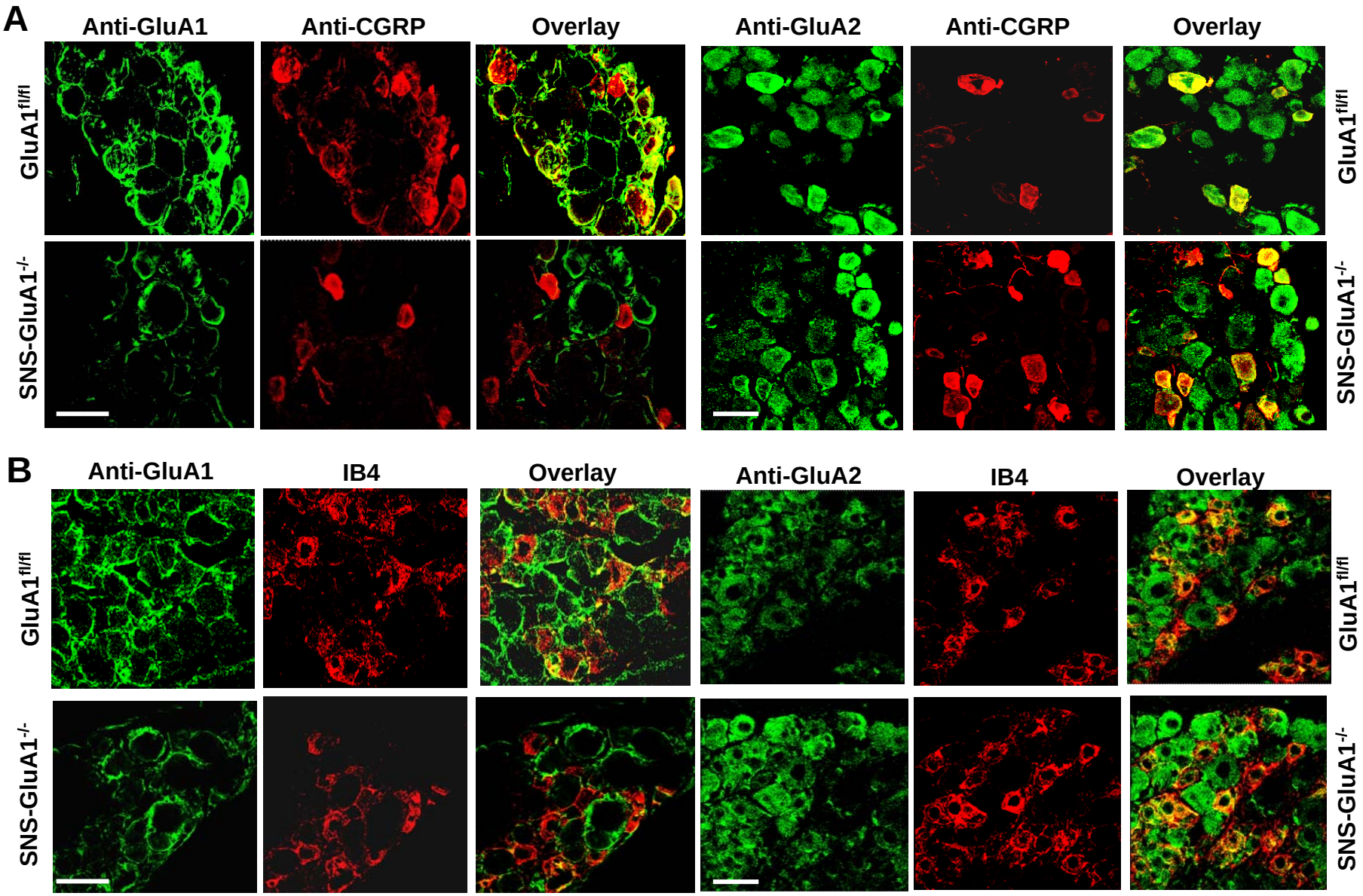

Supplementary figure 1

Supplementary Figure 2: Detailed characterisation of nociceptor-specific deletion mutants of GluA1 and GluA2. Immunohistochemical characterisation of the expression of GluA2 in non-peptidergic nociceptors (CGRP-positive, panel A) and peptidergic nociceptors (IB_4-positive, panel B) in SNS-GluA2$^{-/-}$ mice and the corresponding GluA2$^{fl/fl}$ controls. Western blot analysis (panel C) demonstrates that expression of GluA1 is not altered in SNS-GluA2$^{-/-}$ mice and that of GluA2 is not altered in SNS-GluA1$^{-/-}$ mice. **(D) Stereological analysis reveals that the number of nociceptive neurons (peptidergic and non-peptidergic) in the DRG is comparable between** SNS-GluA1$^{-/-}$ **mice and GluA1$^{fl/fl}$ mice.**

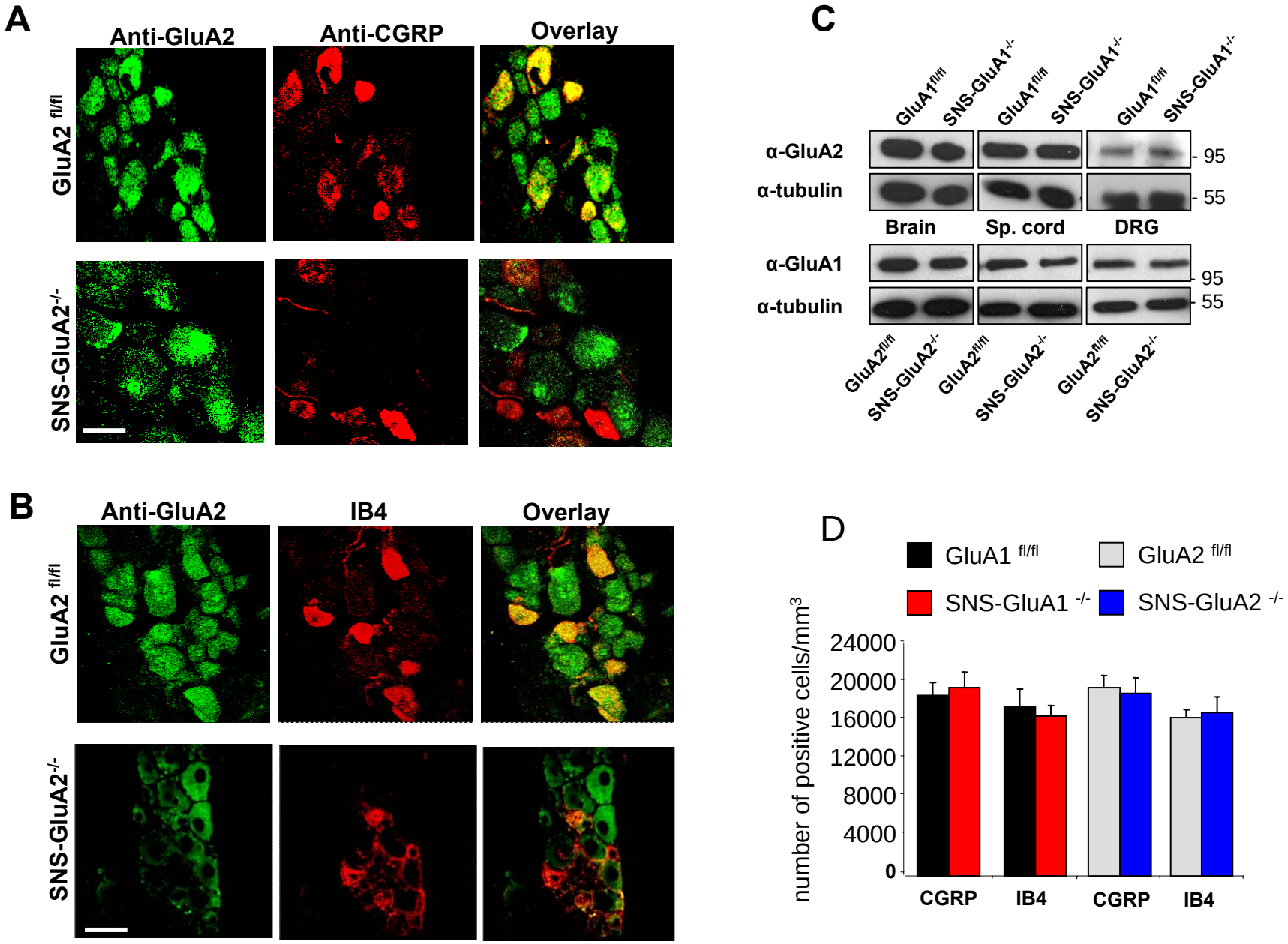

Supplementary figure 2

Supplementary Figure 3: Normal development of the DRG neurons and their peripheral and central spinal terminals in SNS-GluA1$^{-/-}$ and SNS-GluA2$^{-/-}$ mice. A. Peptidergic nociceptors positive for Calcitonin-gene related peptide (CGRP, green) and nonpeptidergic nociceptors binding to isolectin-B_4 (IB_4, red) in DRG and their respective terminals in the spinal dorsal horn develop normally in SNS-GluA1$^{-/-}$ and SNS-GluA2$^{-/-}$ mice, as compared to their control littermates (GluA1$^{fl/fl}$ and GluA2$^{fl/fl}$ mice, respectively). B. Normal distribution of peripheral nerves immunopositive for neuronal markers PGP9.5 and CGRP in the glabrous skin of the hind paws in SNS-GluA1$^{-/-}$ and SNS-GluA2$^{-/-}$ mice. C. Synapses of GCRP-positive (a-d) and IB_4-positive (e-h) nociceptive primary afferents onto PSD-95-positive postsynaptic contacts on spinal cord neurons develop normally in SNS-GluA1$^{-/-}$ and SNS-GluA2$^{-/-}$ mice. Scale bars represent 50μm for DRG (panel A), 100 μm for spinal cord (panel A) as well as skin (panel B) and 2 μm in panel C.

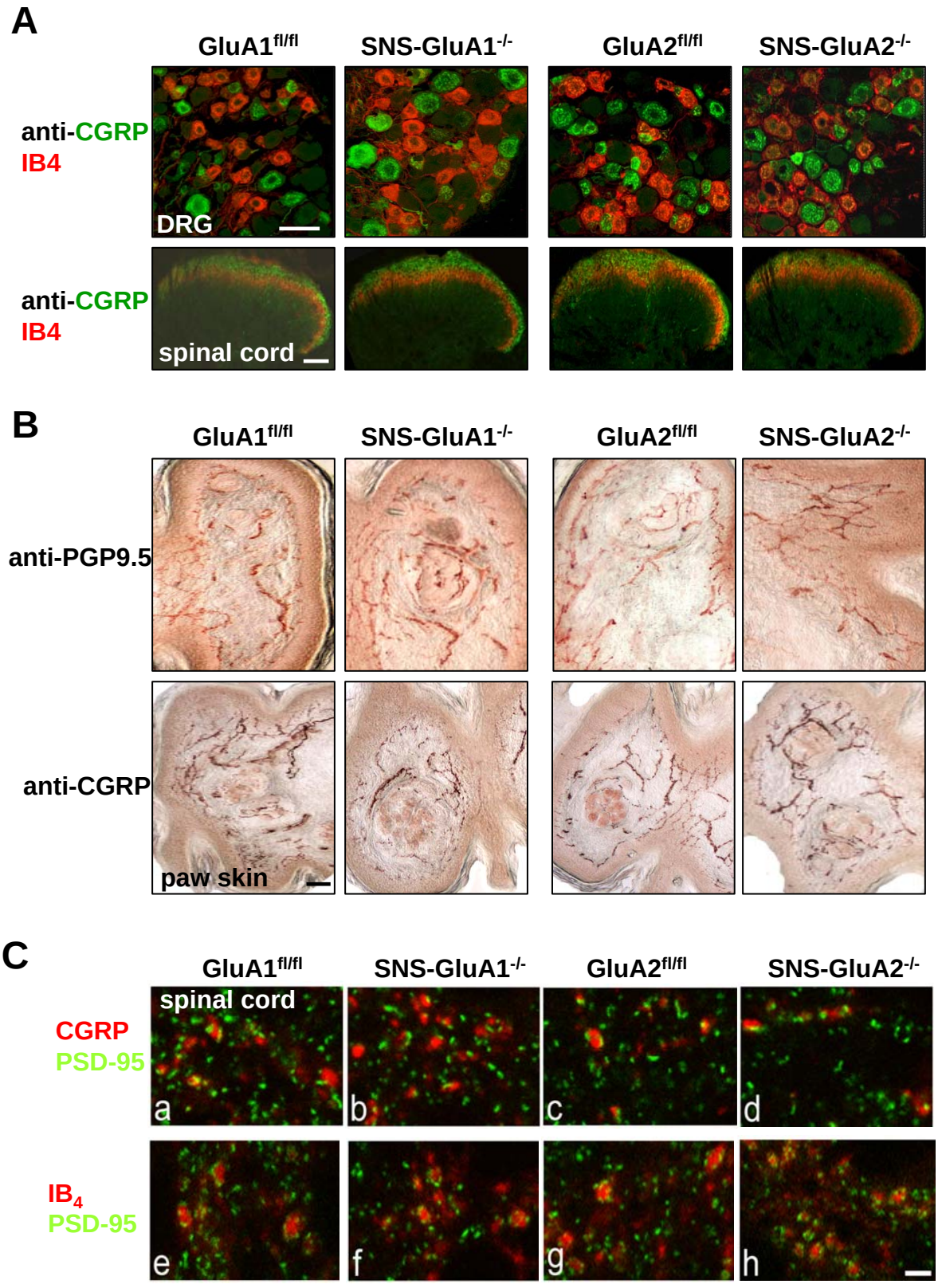

Supplementary figure 3

Supplementary Figure 4: Analysis of acute nociception, early nociceptive hypersensitivity and post-inflammatory hyperalgesia is unchanged in SNS-GluA2$^{-/-}$ in comparison with their control GluA2$^{fl/fl}$ littermates. A & B. Latency of paw withdrawal following application of noxious heat (panel A) and threshold of paw withdrawal to mechanical stimuli applied via the dynamic aesthesiometer (panel B) is normal in SNS-GluA2$^{-/-}$. C & D. SNS-GluA1$^{-/-}$ mice show a normal duration of acute nocifensive behaviours in seconds (s) upon hindpaw intraplantar injection of 0.06% capsaicin (panel C) or 1 % formalin (panel D), during the first 10 minutes (phase I) and 10-50 minutes (phase II) (n = 7-15 mice per group). E & F. In a model of unilateral hindpaw inflammation caused by intraplantar injection of Complete Freund's adjuvant (CFA), SNS-GluA1$^{-/-}$ mice (n = 12) and GluA2$^{fl/fl}$ littermates (n = 12) develop comparable levels of mechanical hypersensitivity and thermal hyperalgesia. D. Summary of response thresholds (defined as a force eliciting a response frequency of at least 40%) to plantar von Frey hair application prior to and at 4 h, 12 h, 24 h and 48 h following intraplantar injection in the above groups of mice. E. Changes in paw withdrawal latency to infrared heat in the inflamed paw represented as percent decrease over the contralateral uninflamed paw prior to and following intraplantar injection of CFA are shown. All data points represent mean ± S.E.M. Behaviour was comparable across the different genotypes ($p > 0.05$, ANOVA, post-hoc Fisher's test, n = 10-12 mice per genotype).

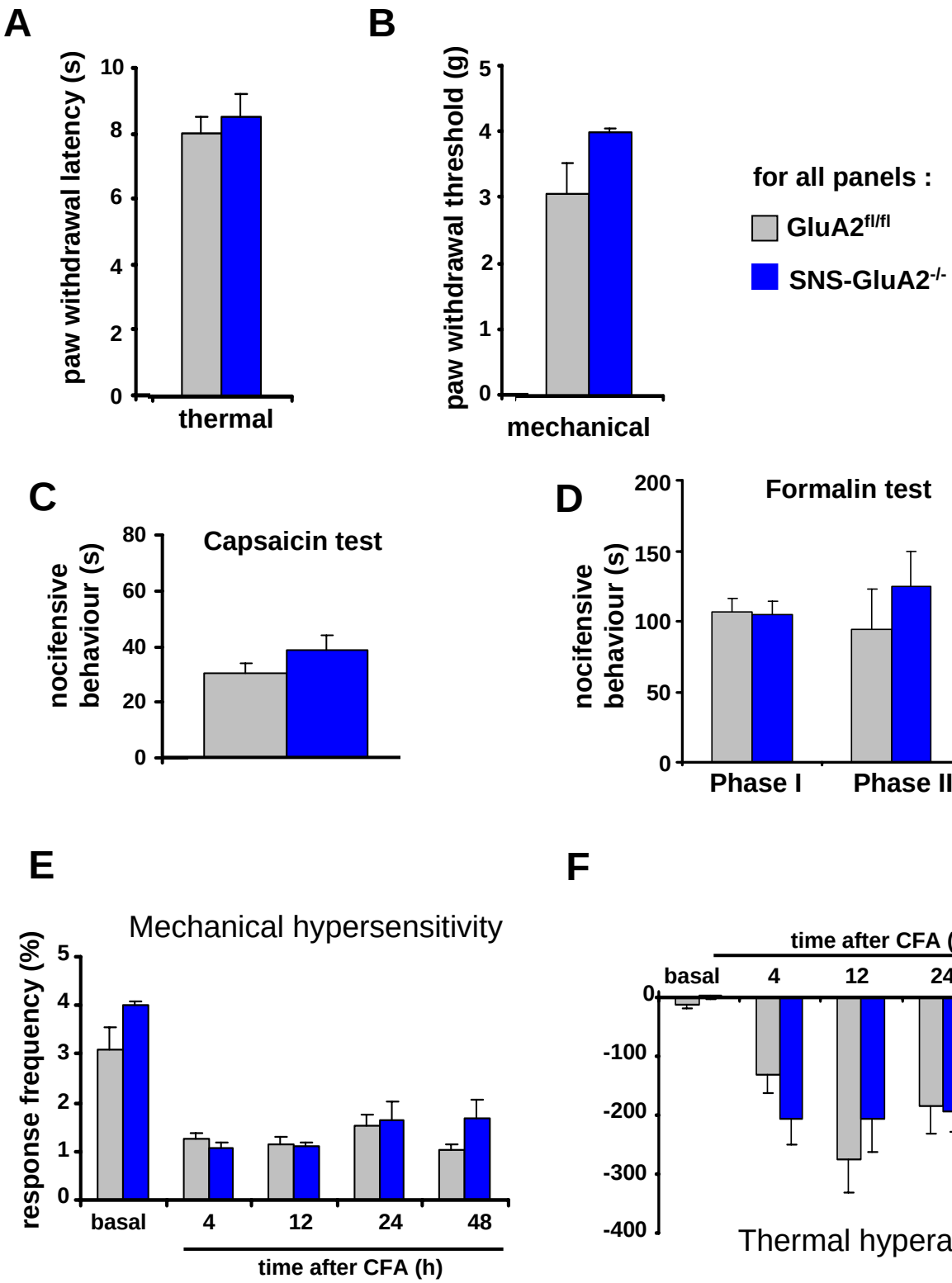

Supplementary figure 4

Supplementary Figure 5: Estimation of the degree of edema and inflammation induced in models of inflammatory pain. A & B. Paw volume was measured using fine calipers before (basal) and at 24 and 48 hours (h) following injection of Complete Freund's adjuvant (CFA) in SNSGluA1$^{-/-}$ mice and their GluA1$^{fl/fl}$ littermates (A), as well as in SNS-GluA1$^{-/-}$ animals and GluA2$^{fl/fl}$ controls (B). C. Comparable knee edema in SNS-GluA1$^{-/-}$ and GluA1$^{fl/fl}$ mice as judged by measuring the circumference of the knee joint (in mm) before (basal) and after kaolin injection. All data points represent mean ± S.E.M. FA- and kaolin-induced oedema was comparable across the different genotypes ($p > 0.05$, ANOVA, post-hoc Fisher's test, n = 10-12 mice per genotype).**(D) Levels of myeloperoxidase, an inflammatory indicator protein, in the synovial membrane increased following knee arthritis to a similar degree in SNS-GluA1$^{-/-}$ and GluA1$^{fl/fl}$ mice (* $P < 0.05$ as compared to the basal state). (E) Immunoreactivity for the neutrophil marker protein, GR1, in the synovial membrane increased following the induction of arthritis (central panel and right panel) to a similar degree in SNS-GluA1$^{-/-}$ and GluA1$^{fl/fl}$ mice as compared to the naïve state (left panel). Arrowheads indicate stained neutrophils in focus and arrows indicate those outside of the focal plane in the images shown. Scale bar represents 100 µM.**

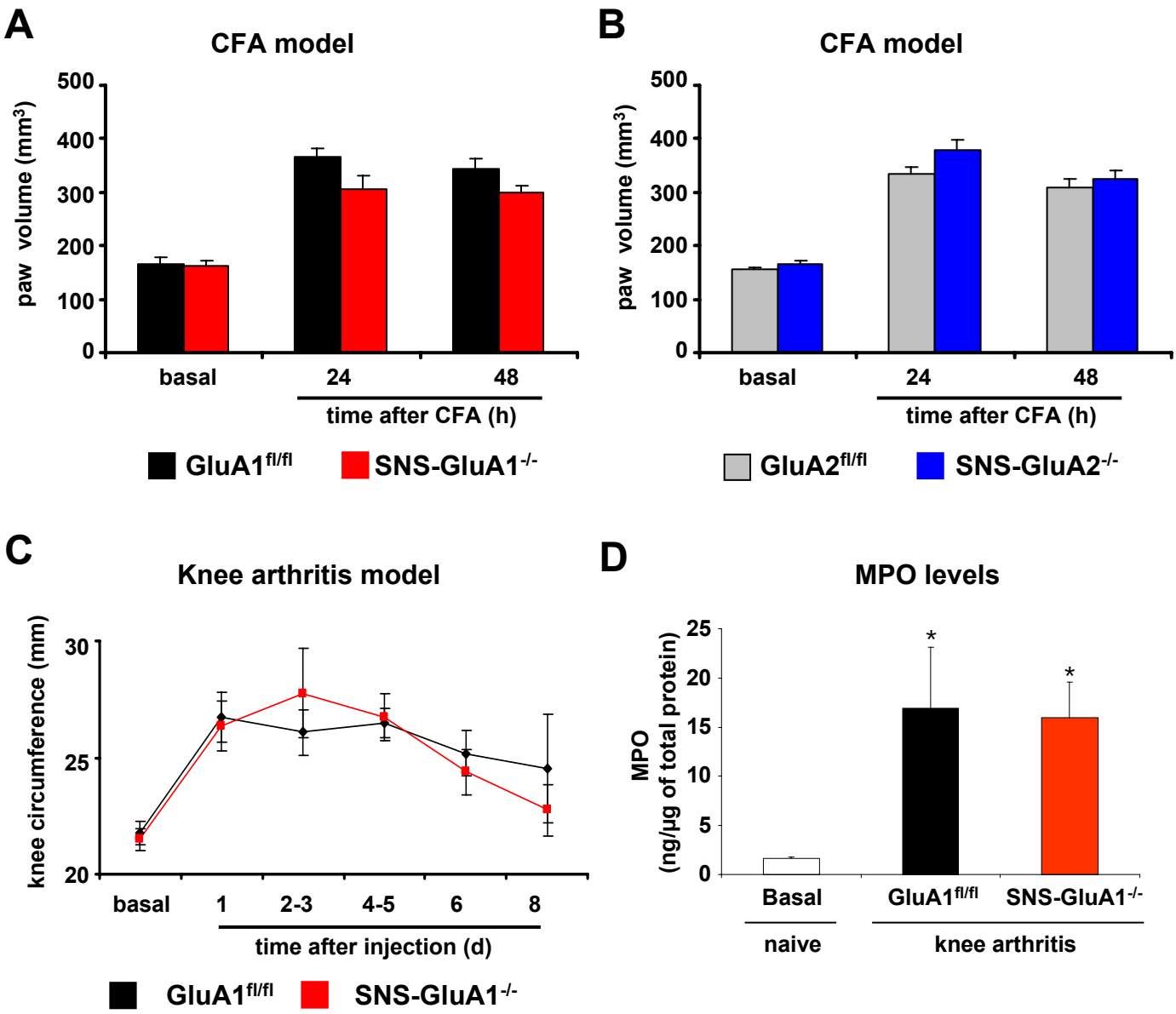

E

α-GR1 (neutrophil marker)

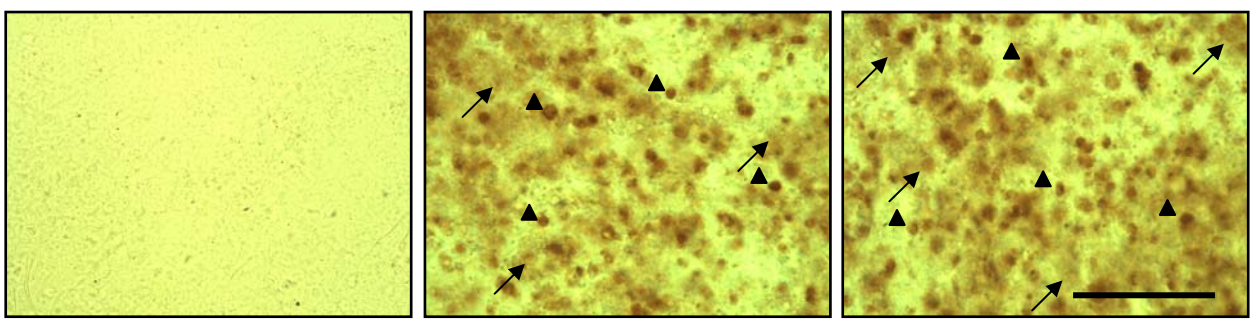

Supplementary figure 5

Supplementary Figure 6: Analysis of responses of firing frequency of A-ð-type mechanoceptors (AM) evoked by application of pressure via a nanomotor (expressed in terms of displacement) following CFA-induced inflammation (inflamed) over the naïve state (basal) in GluA1$^{fl/fl}$ mice and SNS-GluA1$^{-/-}$ mice. $P > 0.05$ between genotypes, repeated measures ANOVA over the whole curve; n = 10-20 mice per group.

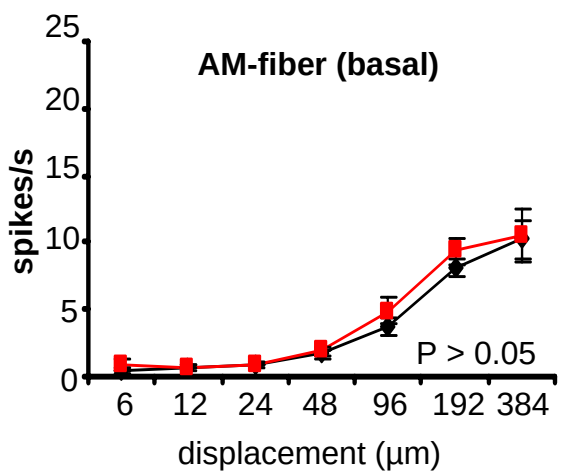

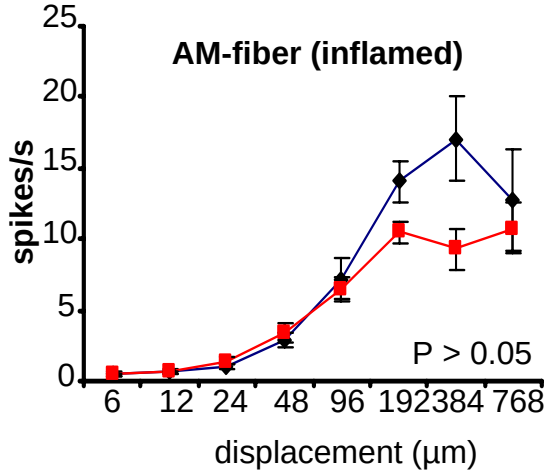

Supplementary figure 6

Supplementary Figure 7: Effects of a specific antagonist of calcium-permeable 1-napthyl spermin (1-NAS, 1 nmol, intraplantar injection) on peripheral glutamate-induced hyperalgesia. Glutamate significantly induced mechanical hyperalgesia in GluA1$^{fl/fl}$ mice (*p = 0.004 as compared to basal mechanical value at all von Frey intensities) and to a significantly lesser extent in SNS-GluA1$^{-/-}$ mice (*p = 0.048 as compared to basal at 0.6g and 1g; δ p < 0.01 as compared to GluA1$^{fl/fl}$ mice). 1-NAS significantly reduced glutamate-induced mechanical hyperalgesia in GluA1$^{fl/fl}$ mice († p < 0.01 as compared to vehicle treated group) in contrast, treatment with 1-NAS did not further affect responses in SNS-GluA1$^{-/-}$ mice (p = 0.35 between glutamate + vehicle and glutamate + 1-NAS). ANOVA followed by post-hoc Fisher's test; n = 5 mice per group.

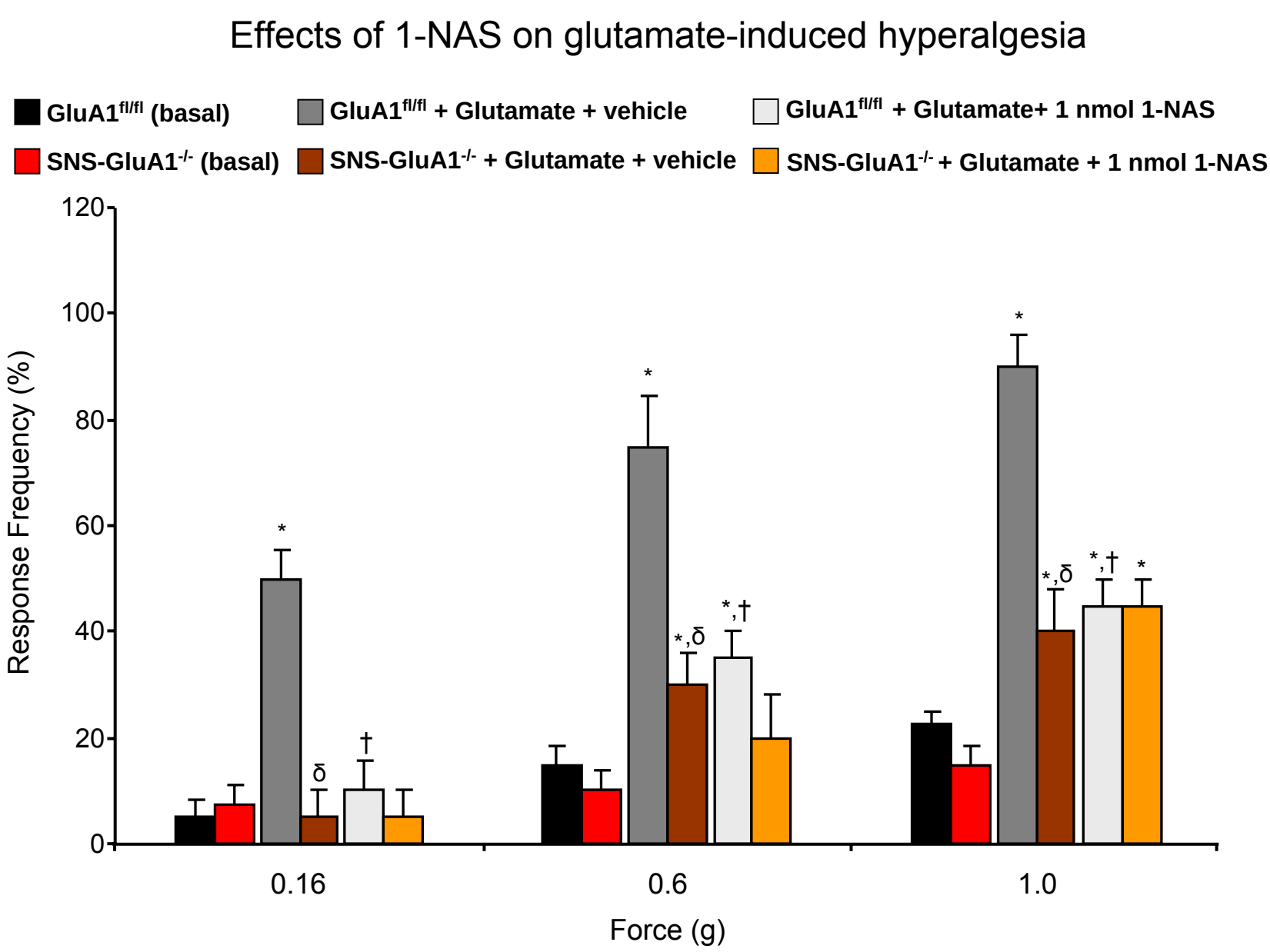

* $p < 0.05$ as compared to basal; † $p < 0.01$ as compared to vehicle group; δ $p < 0.01$ as compared to GluA1$^{fl/fl}$

Supplementary figure 7

Supplementary Figure 8: Analysis of glutamate levels in the spinal dorsal horn via microdialysis prior to and following intraplantar formalin injection in the paw. (A) Schematic view of the placement of a microdialysis probe within the spinal dorsal horn of mice *in vivo* (see methods for details) to estimate glutamate concentrations in the spinal dorsal horn of SNS-GluA1$^{-/-}$ (n = 10) and GluA1$^{fl/fl}$ (n = 10) mice. (B) Glutamate concentration in the dialysate of SNS-GluA1$^{-/-}$ and GluA1$^{fl/fl}$ mice before (left side, values on x-axis < 0) and after (right side, values on x-axis > 0) intraplantar formalin injection in the hindpaw (arrow). (C) For comparison of time courses of glutamate concentrations in dialysates, the area under the concentrations versus time curve (AUC) was calculated employing the linear trapezoidal rule. AUCs were subsequently submitted to ANOVA for repeated measurements using the within subject factor time and the between subject factor genotype. To assess differences in the immediate and sustained glutamate release the time after formalin was split in 0-25 min and 30-55 min bin. * p < 0.05.

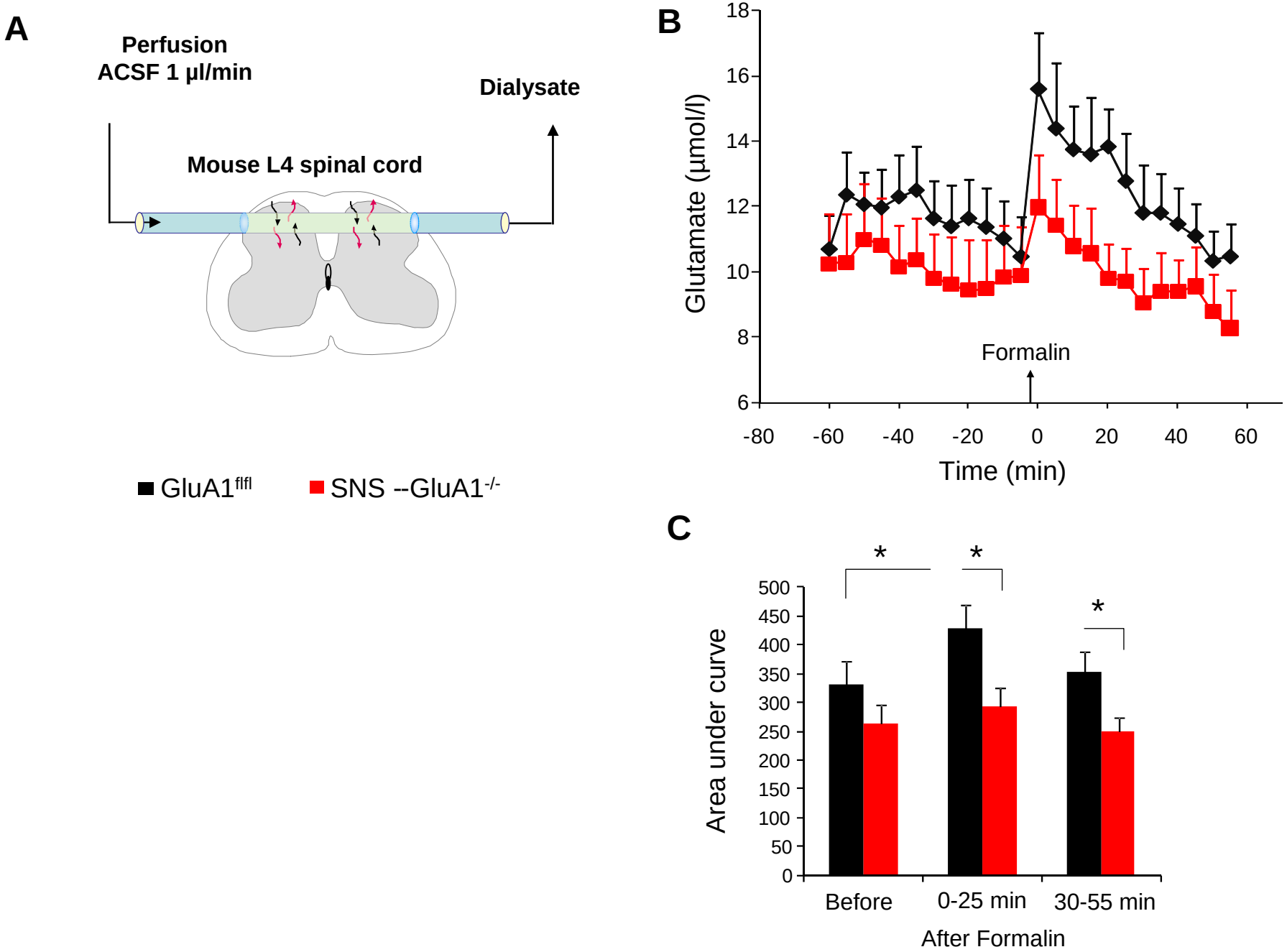

Supplementary figure 8

Supplementary Figure 9: Motor performance as judged in the open-field test was not altered upon systemic or peripheral injection of GYKI 52466. The number of line crosses was taken as an indication of horizontal activity, whereas the number of rearings represented vertical activity in these animals (n = 6-10 mice/group).

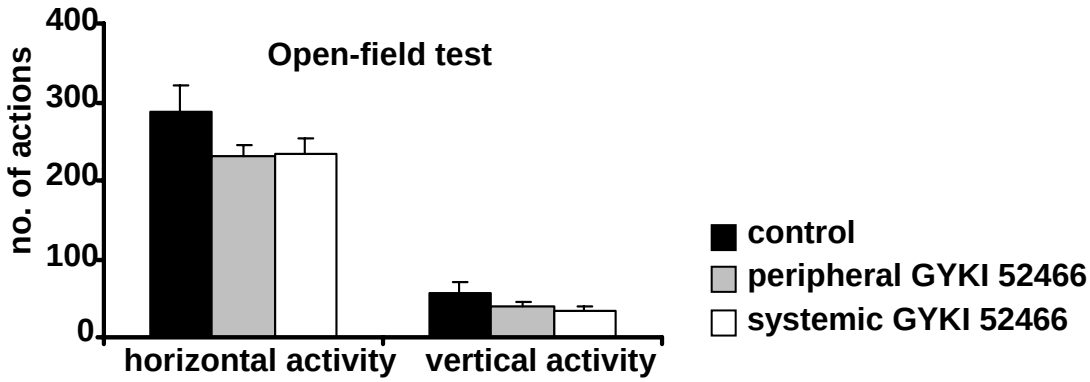

Supplementary figure 9

Supplementary table 1: Analysis of synaptic connections formed by peptidergic (CGRP-positive) and isolectin-B4 binding non-peptidergic (BSI-B4) fibers in mutant mice and their respective control littermates.

	CGRP		BSI-B4	
	% boutons with contacts	**mean contacts per bouton**	**% boutons with contacts**	**mean contacts per bouton**
GluA1$^{fl/fl}$	89	1.76	98	3.27
SNS-GluA1$^{-/-}$	92	1.97	98	3.57
GluA2$^{fl/fl}$	91	1.99	94	3.08
SNS-GluA2$^{-/-}$	90	1.82	100	2.91

Supplemetary table 2. The physiological properties of individual primary afferent nociceptors recorded in GluA$^{fl/fl}$ and SNS-GluA$^{-/-}$mice. The average conduction velocity and median von Frey thresholds for AM and C-fiber nociceptors recorded in the current experiment were listed above. These two parameters were neither different between two genotypes nor changed before and after inflammation in genotype (Student's t-test, $P > 0.05$).

	GluA$^{fl/fl}$				**SNS-GluA$^{-/-}$**			
	Before inflammation		**After inflammation**		**Before inflammation**		**After inflammation**	
AM-fibers	CV m/s	vFT (mN)	CV m/s	vFT (mN)	CV m/s	vFT (mN)	CV m/s	vFT (mN)
	4.52±0.48 n=13	3.3 (1.4-10)	5.09±0.61 n=17	3.3 (1.4-10)	4.22±0.59 n=10	3.3 (1.4-3.3)	3.61±0.51 n=19	3.3 (1-6.3)
C-fibers	0.52±0.03 n=28	3.3 (1-6.3)	0.55±0.04 n=21	3.3 (1.4-6.3)	0.51±0.03 n=16	3.3 (1-6.3)	0.46±0.03 n=22	3.3 (1.4-10)